Myocyte differentiation generates nuclear invaginations traversed by myofibrils associating with sarcomeric protein mRNAs

Tomoyuki Abe[1,2], Kazunori Takano[1,2], Akiko Suzuki[1], Yutaka Shimada[3], Masaki Inagaki[4], Naruki Sato[1], Takashi Obinata[1] and Takeshi Endo[1,2,*]

[1]Department of Biology, Faculty of Science, and Graduate School of Science and Technology, Chiba University, Yayoicho, Inageku, Chiba, Chiba 263-8522, Japan
[2]CREST, Japan Science and Technology Agency (JST), Kawaguchi, Saitama 332-0012, Japan
[3]Department of Anatomy, Chiba University School of Medicine, Chuoku, Chiba, Chiba 260-8670, Japan
[4]Division of Biochemistry, Aichi Cancer Center Research Institute, Nagoya, Aichi 464-8681, Japan
*Author for correspondence (e-mail: t.endo@faculty.chiba-u.jp)

Accepted 30 September 2004
Journal of Cell Science 117, 6523-6534 Published by The Company of Biologists 2004
doi:10.1242/jcs.01574

Summary

Certain types of cell both in vivo and in vitro contain invaginated or convoluted nuclei. However, the mechanisms and functional significance of the deformation of the nuclear shape remain enigmatic. Recent studies have suggested that three types of cytoskeleton, microfilaments, microtubules and intermediate filaments, are involved in the formation of nuclear invaginations, depending upon cell type or conditions. Here, we show that undifferentiated mouse C2C12 skeletal muscle myoblasts had smooth-surfaced spherical or ellipsoidal nuclei, whereas prominent nuclear grooves and invaginations were formed in multinucleated myotubes during terminal differentiation. Conversion of mouse fibroblasts to myocytes by the transfection of *MyoD* also resulted in the formation of nuclear invaginations after differentiation. C2C12 cells prevented from differentiation did not have nuclear invaginations, but biochemically differentiated cells without cell fusion exhibited nuclear invaginations. Thus, biochemical differentiation is sufficient for the nuclear deformation. Although vimentin markedly decreased both in the biochemically and in the terminally differentiated cells, exogenous expression of vimentin in myotubes did not rescue nuclei from the deformation. On the other hand, non-striated premyofibrils consisting of sarcomeric actin-myosin filament bundles and cross-striated myofibrils traversed the grooves and invaginations. Time-lapse microscopy showed that the preformed myofibrillar structures cut horizontally into the nuclei. Prevention of myofibril formation retarded the generation of nuclear invaginations. These results indicate that the myofibrillar structures are, at least in part, responsible for the formation of nuclear grooves and invaginations in these myocytes. mRNA of sarcomeric proteins including myosin heavy chain and α-actin were frequently associated with the myofibrillar structures running along the nuclear grooves and invaginations. Consequently, the grooves and invaginations might function in efficient sarcomeric protein mRNA transport from the nucleus along the traversing myofibrillar structures for active myofibril formation.

Key words: Muscle cell differentiation, Nuclear invaginations, Vimentin, Actin, Myosin, Myofibrils, mRNA transport

Introduction

The nuclei of various types of cells are not always smooth-surfaced spheres or ellipsoids but are occasionally folded, grooved, convoluted or invaginated. For instance, tumor-derived cell lines generally have such irregularly shaped nuclei (Hoshino, 1961; Bernhard and Granboulan, 1963). Nuclear grooves and invaginations also occur in some non-cancerous cell lines including 3T3 and NRK cells (Fricker et al., 1997; Clubb and Locke, 1998). The nuclear deformation is not restricted to these cultured cells but is detected in some cell types in vivo. The nuclei of striated and smooth muscle cells as well as those of liver cells in tissues are also convoluted or invaginated (Lane, 1965; Franke and Schinko, 1969; Bourgeois et al., 1979). Moreover, not only animal cells but also certain plant cells such as onion epidermal cells and cultured tobacco cells have nuclear grooves and invaginations (Collings et al., 2000). The number and nature of invaginations vary from cell type to cell type, ranging from simple invaginations to intricate branched structures that penetrate into or entirely traverse the nucleus. The occurrence of nuclear grooves and invaginations in a wide variety of cell types may imply their general functional significance.

Several tumor cells including human pancreatic carcinoma MIA PaCa-2 cells have nuclear invaginations and lobules containing well-developed perinuclear rings composed of vimentin and keratin intermediate filaments (IFs) (Kamei, 1994). These filaments run along deep invaginations in the nucleus and form closed rings around the invaginations and constrictions. Thus, these perinuclear IFs are postulated to be involved in the formation of nuclear invaginations and lobules in these cells. By contrast, human adrenal cortex carcinoma

SW-13 cells lacking vimentin are characterized by large folds or invaginations, whereas cells expressing vimentin have regular or smooth nuclei (Sarria et al., 1994). Forced expression of vimentin in cells lacking vimentin restores the smooth nuclear shape, but mutated vimentin expression in the cells with endogenous vimentin disrupts the organization of vimentin filaments and results in invaginated nuclei (Sarria et al., 1994). Although these two results are contradictory, vimentin-type IFs seem to participate in the determination of nuclear shape in these cells.

During nuclear envelope breakdown in mitosis, early spindle microtubules penetrate into the nuclei to cause nuclear folds and invaginations. These microtubules create mechanical tension and induce tearing of the nuclear lamina, which underlies the inner nuclear membrane and stabilizes the nuclear envelope. The tearing of the nuclear lamina in consequence leads to nuclear envelope breakdown (Georgatos et al., 1997; Beaudouin et al., 2002; Salina et al., 2002).

3T3 cells have two types of nuclear invagination: branched invaginations radiating horizontally to the substrate and invaginations running vertically to the substrate (Clubb and Locke, 1998). The former invaginations contain actin filaments presumably associated with the cytoplasmic face of the nuclear membrane. Onion epidermal cells contain prominent actin filament bundles in the nuclear grooves and invaginations (Collings et al., 2000). Accordingly, any one of the three types of cytoskeleton, IFs, microtubules and actin microfilaments, seems to be responsible for the formation of nuclear grooves and invaginations, depending on cell type and physiological or pathological states. Furthermore, convoluted or invaginated nuclei of striated and smooth muscle myofibers are proposed to be generated either by mechanical forces through muscle contraction (Lane, 1965) or by intracellular ion changes (Franke and Schinko, 1969). Therefore, the nuclear deformation in various cell types may not be explained by a unified mechanism.

Several proposals have been made for the functional significance of nuclear grooves and invaginations. As nuclear grooves and invaginations substantially increase the surface area of the nucleus, they might function in nucleocytoplasmic transport such as mRNA export from the nucleus to the cytoplasm and protein import from the cytoplasm to the nucleus (Fricker et al., 1997; Collings et al., 2000). Alternatively, these structures might contribute to the release of Ca^{2+} into the nucleus from the nuclear envelope, which serves as a Ca^{2+} store, and may consequently be responsible for Ca^{2+} signaling in the nucleus, including gene expression (Lui et al., 1998). However, the functions of these structures remain to be elucidated.

Here we report that nuclear grooves and invaginations were formed during both biochemical and terminal differentiation of the mouse C2C12 skeletal muscle cells. Although vimentin expression was downregulated during differentiation, forced expression of vimentin in myotubes did not restore smooth nuclear shape. On the other hand, premyofibrils and myofibrils containing sarcomeric actin and myosin cut into the nuclei to form nuclear invaginations. Sarcomeric protein mRNAs were associated with these myofibrillar structures. Thus, the invaginations seem to provide the efficient translocation of these mRNAs from the nuclei to the nascent myofibrils.

Materials and Methods

Cell culture

Mouse C2C12 skeletal muscle cells (Blau et al., 1983) derived from C2 cells (Yaffe and Saxel, 1977) were cultured as described previously (Endo, 1992). The proliferating myoblasts were maintained in Dulbecco's modified Eagle's medium (DMEM) supplemented with 10% fetal bovine serum (FBS) (growth medium). To induce terminal differentiation, the growth medium was replaced with DMEM supplemented with 5% horse serum (differentiation medium) and cells were maintained for 96 hours. To inhibit terminal differentiation, 5 mM sodium butyrate or 2% dimethyl sulfoxide (DMSO) was included in the differentiation medium (Endo and Nadal-Ginard, 1987). To impair myofibrillogenesis, 10 mM 2,3-butanedione monoxime (BDM) (Sigma) or 12 mM KCl were added to the differentiation medium (Bandman and Strohman, 1982; Soeno et al., 1999). Mouse C3H/10T1/2 (10T1/2) fibroblasts (Reznikoff et al., 1973) were cultured in the growth medium.

Transfection

Mouse *MyoD* cDNA in pBluescript (Stratagene) was a gift from Dr Andrew Lassar. It was transfected to 10T1/2 cells by the calcium phosphate-mediated method (Endo, 1992). Mouse *vimentin* cDNA (Wood et al., 1989) (American Type Culture Collection) was subcloned in pRc/CMV (Invitrogen). The recombinant plasmid pCMV/Vim was transfected to C2C12 myoblasts, and stable transfectants were selected in the growth medium containing 400 μg/ml Geneticin (G418) (Sigma).

Northern blotting

Cytoplasmic RNA was prepared from the cells and northern blotting was carried out as described previously (Endo and Nadal-Ginard, 1987). The 0.8-kb *Hin*dIII fragment of pCMV/Vim was labeled with [α-^{32}P]dCTP (>111 TBq/mmol, ICN Biomedicals) using a BcaBEST labeling kit (Takara Shuzo) and hybridized with RNA transferred onto nitrocellulose filters.

Preparation of antibodies

A MyoD-specific 25mer peptide corresponding to the amino acids 58-82 (KPEEHAHFSTAVHPGPGAREDEHVR) of mouse MyoD (Davis et al., 1987) was synthesized with MilliGen/Biosearch PepSynthesizer 9050 and purified by reverse-phase chromatography with a Waters DeltaPrep 4000 equipped with an Inertsil ODS-2 column (GL Science Co). 1 mg peptide was emulsified with Freund's complete adjuvant and injected into a New Zealand white rabbit. Second and third immunizations with 0.5 mg of the peptide emulsified with Freund's incomplete adjuvant were made 40 and 70 days after the first injection, respectively. The whole blood was collected 18 days after the third injection, and the IgG fraction was purified with Protein G Sepharose 4 Fast Flow (Amersham Biosciences). Purified chicken gizzard actin (Endo and Masaki, 1982) was subjected to SDS-PAGE, and its protein band was excised from the gel and mashed. It was injected into a rabbit as for the MyoD peptide. The antibody was purified by affinity chromatography using CNBr-activated Sepharose 4B (Amersham Biosciences) coupled with gizzard actin. The purified antibody was absorbed with chicken skeletal muscle actin as described previously (Endo and Masaki, 1984).

Fluorescence microscopy

Cells cultured on glass coverslips were processed for immunofluorescence microscopy as described previously (Endo and Nadal-Ginard, 1998). Primary antibodies used were the monoclonal antibodies (mAbs) MF20 (Bader et al., 1982) to muscle-specific myosin heavy chain (MyHC); A4.1025 to sarcomeric MyHC (Webster

et al., 1988) (Developmental Studies Hybridoma Bank); KT55 to mouse vimentin (Inagaki et al., 1996); mAbs to human nucleoporin p62 (BD Transduction Laboratories), mouse kinesin heavy chain (Chemicon International) and mouse dynein (Chemicon International); and the polyclonal antibodies (pAbs) to MyoD peptide and to gizzard actin. Fluorescein isothiocyanate (FITC)-conjugated (Cappel Laboratories) or Alexa 488-conjugated (Molecular Probes) goat anti-mouse IgG and anti-rabbit IgG were used as secondary antibodies. Actin filaments were detected by the staining with rhodamine-phalloidin or Alexa 488-phalloidin (Molecular Probes). The nuclei and the endoplasmic reticulum (ER) were counterstained with 1 μg/ml bisbenzimide H33258 (Hoechst 33258) (Roche) and 2.5 μg/ml $DiOC_6(3)$ (Molecular Probes), respectively. The specimens were observed with a Zeiss Axioskop microscope or with a Zeiss LSM 410 confocal laser-scanning microscope.

Time-lapse microscopy

Mouse skeletal muscle *α-actin* cDNA (1.1 kb) was cloned by reverse transcription (RT)-PCR from poly(A)$^+$ RNA prepared form C2C12 myotube cytoplasmic RNA. The cDNA was subcloned in pEGFP-C1 vector (BD Biosciences Clontech) and transfected to C2C12 myoblasts cultured on glass base dishes (Iwaki) by using FuGENE 6 Transfection Reagent (Roche Molecular Biochemicals). The transfected cells were cultured in the differentiation medium for 24 hours and in fresh differentiation medium for a further 48 hours. Most cells differentiated to form myotubes by the end of this incubation. The nuclei of these cells were stained with 1 μg/ml Hoechst 33342 (Sigma) in serum-free DMEM for 5 minutes. The cells were then cultured in differentiation medium at 37°C in a Zeiss CO_2 incubator CZI-3 and observed with a Zeiss Axiovert 200 microscope equipped with an incubator. EGFP-actin and H33342 fluorescence was recorded at intervals of 20-30 minutes.

Electron microscopy

Cells cultured on carbon-coated glass coverslips were fixed with 2.5% glutaraldehyde in 0.1 M sodium phosphate buffer (pH 7.2) at room temperature, postfixed with 1% OsO_4 in the same buffer at 4°C, and en bloc stained with 0.5% uranyl acetate in 50 mM maleate buffer (pH 5.2) for 1 hour at room temperature. They were dehydrated in an ascending ethanol series, treated in propylene oxide, and embedded in Epon 812. Thin sections were collected on carbon-coated, collodion-covered grids and stained with uranyl acetate and lead citrate. The specimens were examined with a JEM-1200EX II electron microscope (JEOL) at an accelerating voltage of 80 kV.

Fluorescent in situ hybridization (FISH)

Mouse embryonic fast skeletal muscle *MyHC* (*MyHC3*) cDNA (6 kb) was cloned from the C2C12 myotube cDNA library constructed in λZAPII (Matsumoto et al., 1997) by screening with the mAb A4.1025. *MyHC* and *α-actin* cDNAs were subcloned in pBluescript II vector (Stratagene). Sense and antisense in vitro transcripts were synthesized with T3 and T7 RNA polymerases (Promega) in the presence of digoxigenin (DIG)-11-UTP (Roche). C2C12 myotubes cultured on glass coverslips were fixed with 4% paraformaldehyde in 0.1 M sodium phosphate buffer (pH 7.4) for 15 minutes. The sense and antisense probes were hybridized with the fixed myotubes as described (Bassell et al., 1998). After washing, the cells were incubated with rhodamine-conjugated anti-DIG sheep IgG Fab fragment (Roche) in a staining buffer (0.5 M NaCl, 50 mM Tris-HCl, pH 8.0, 1% bovine serum albumin and 0.1% Triton X-100) for 1 hour, and then with Alexa 488-phalloidin in the staining buffer for 20 minutes. They were washed three times with the staining buffer and observed with a confocal laser-scanning microscope.

Results

Both terminally and biochemically differentiated myocytes have invaginated nuclei

When the interphase nuclei of exponentially growing C2C12 myoblasts were observed by phase-contrast microscopy and bisbenzimide H33258 staining, they were smooth-surfaced ellipsoids as observed in many other types of cultured cells (Fig. 1A a,b). If the myoblasts were shifted to differentiation medium, they terminally differentiated to form multinucleated myotubes. The myotubes were fully developed by day 4. Both

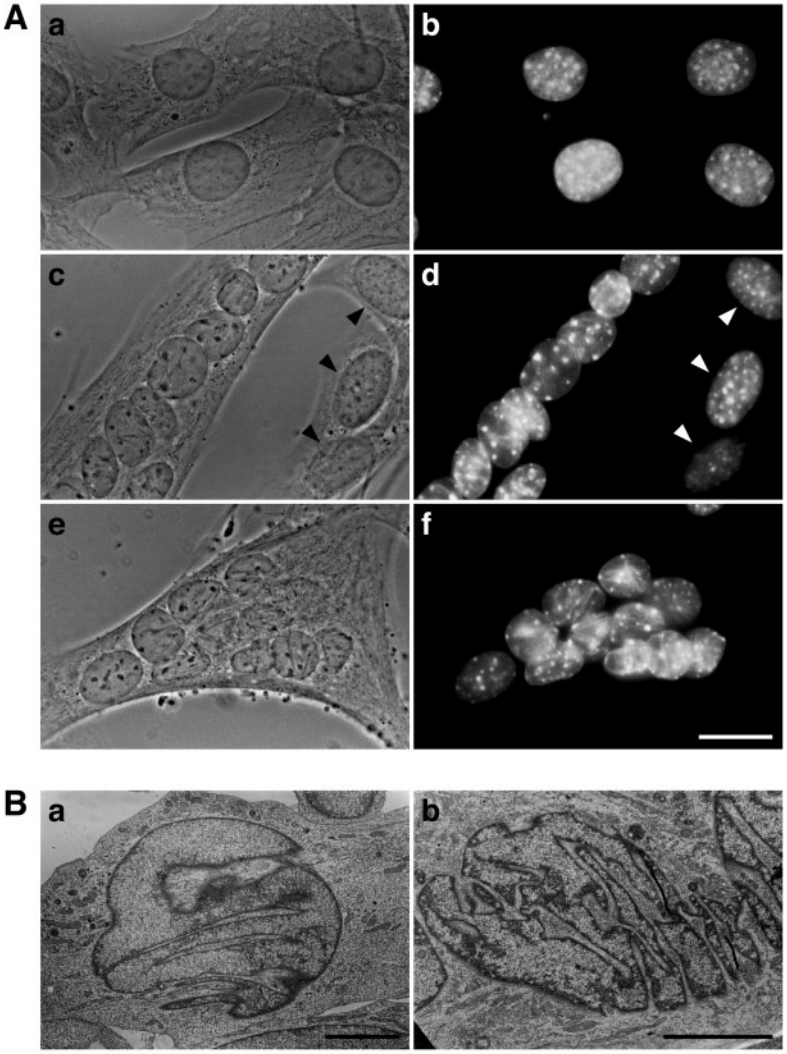

Fig. 1. Nuclear shape of C2C12 myoblasts and myotubes. C2C12 myoblasts were cultured in the growth medium for 1 day, and myotubes were formed by culturing for 4 days in the differentiation medium. (A) Phase-contrast images (a,c,e) and corresponding bisbenzimide H33258-stained images (b,d,f) of myoblasts (a,b) and myotubes (c-f). Arrowheads indicate the smooth nuclei of residual myoblasts in the myotube culture (c,d). (B) Electron micrographs of myotube nuclei. Bar, 20 μm (A); 5 μm (B).

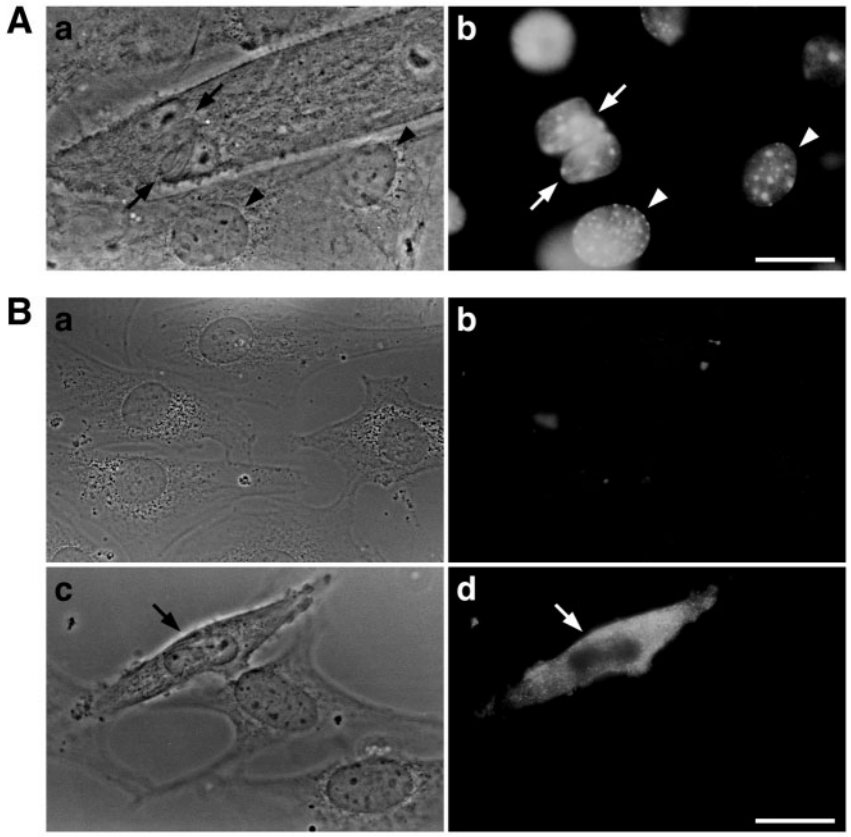

Fig. 2. Nuclear shape of 10T1/2 myotubes and biochemically differentiated C2C12 cells. (A) Phase-contrast image (a) and corresponding H33258-stained image (b) of a 10T1/2 myotube. 10T1/2 fibroblasts were transfected with *MyoD* and maintained for 4 days in the differentiation medium. Arrows indicate myotube nuclei with invaginations. Arrowheads indicate smooth nuclei in mononucleated cells. (B) Phase-contrast images (a,c) and corresponding immunofluorescent images detecting muscle-specific MyHC (b,d) of sodium butyrate-treated (a,b) or DMSO-treated (c,d) C2C12 cells. C2C12 myoblasts were cultured for 4 days in the differentiation medium containing either 5 mM sodium butyrate or 2% DMSO. Biochemically differentiated cells were detected by the staining with the mAb MF20 to muscle-specific MyHC. Arrows indicate biochemically differentiated cells with invaginated nuclei. (C) Ratio of smooth-surfaced and grooved or invaginated nuclei. C2C12 Mb, proliferating C2C12 myoblasts. C2C12 Mt, C2C12 myotubes cultured for 4 days in the differentiation medium. C2C12(DMSO), MyHC-positive biochemically differentiated C2C12 cells cultured for 4 days in the differentiation medium containing DMSO. C2Vm8 Mt, C2Vm8 myotubes cultured for 4 days in the differentiation medium. More than 200 nuclei were counted in each experiment. The values are the mean±s.d. of three experiments. Bar, 20 μm.

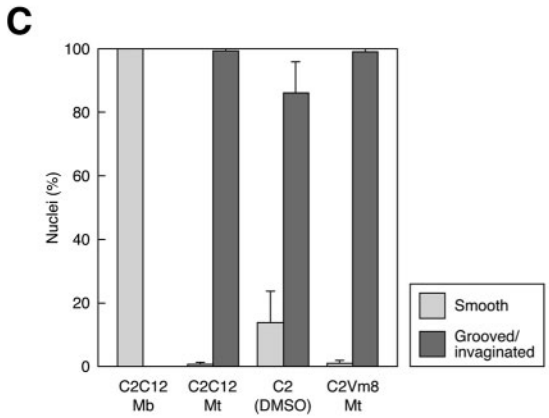

phase-contrast and H33258-stained images revealed that the nuclei in myotubes had prominent grooves or invaginations (Fig. 1A c-f). One nucleus had multiple grooves or invaginations of varying lengths and directions. By contrast, the nuclei in residual myoblasts had a smooth appearance even in the differentiation medium (Fig. 1A c,d, arrowheads). The transition of nuclear shape occurred in an all-or-none fashion, that is, all proliferating myoblasts examined in the growth medium had smooth nuclei, whereas essentially all nuclei in myotubes cultured for 4 days in the differentiation medium had grooves or invaginations (Fig. 2C). Electron microscopy of the myotubes demonstrated that the nuclei had invaginations and deep clefts (Fig. 1B). They often had a segmented or curved maze-like appearance in section. Some invaginations transected the nucleus entirely. All these invaginations and clefts were demarcated by the nuclear envelope, and consequently the nucleoplasm was not exposed to the cytoplasm.

To determine whether the nuclear deformation is a phenomenon specific for C2C12 myotubes, 10T1/2 fibroblasts were transfected with *MyoD* cDNA. This transfection efficiently converted the fibroblasts into myogenic cells, and the transfected cells formed myotubes in the differentiation medium (Fig. 2A a) as has been reported (Davis et al., 1987). MyoD was expressed in the myotube nuclei but not in the mononucleated untransfected cells as revealed by immunofluorescence microscopy (data not shown). The MyoD-expressing nuclei in the myotubes had grooves or invaginations as did the C2C12 myotube nuclei (Fig. 2A, arrows), whereas the nuclei in mononucleated cells were smooth-surfaced (Fig. 2A, arrowheads). Accordingly, the nuclear deformation is not specific for C2C12 myotubes but likely to take place ubiquitously in terminally differentiated myogenic cells.

We examined whether cell fusion is required for the nuclear deformation. When rat L6E9 cells are cultured in differentiation medium containing certain differentiation-blocking agents including DMSO or sodium butyrate, the cells are prevented from biochemical differentiation, and in consequence terminal differentiation is aborted (Endo and Nadal-Ginard, 1987). C2C12 myoblasts were incubated in the differentiation medium supplemented with 5 mM sodium butyrate. They did not fuse to form myotubes, and their nuclear surface remained smooth for at least 4 days (Fig. 2B a and Fig. 3C a). These cells did not differentiate biochemically as

revealed by immunostaining with mAb MF20 that recognizes muscle-specific MyHC (Fig. 2B b). Next, C2C12 myoblasts were cultured in the differentiation medium containing 2% DMSO. Essentially all cells were mononucleated at day 4, but morphologically two types of cells were discriminated. More than 90% of the cells were flat and the rest were refractile (Fig. 2B c and Fig. 3C c, arrows). The former type of cell had smooth-surfaced nuclei and did not express muscle-specific MyHC (Fig. 2B c,d). By contrast, the latter biochemically differentiated to express muscle-specific MyHC (Fig. 2B c,d, arrows), and ~85% contained grooved or invaginated nuclei (Fig. 2C). These results imply that the biochemically differentiated state, even without cell fusion, is sufficient for nuclear deformation. As neither of these biochemically differentiated cells nor the myotubes at this stage contracted, the possibility that contraction is responsible for the nuclear deformation is ruled out.

Downregulation of vimentin during biochemical and terminal differentiation is not correlated with nuclear invagination

During myogenesis of chicken skeletal muscle in vivo and in culture, two types of IF proteins, vimentin and desmin, are differentially expressed (Bennett et al., 1979; Tokuyasu et al., 1984). Vimentin is the sole species of cytoplasmic IF proteins in undifferentiated myoblasts. When myogenic differentiation begins, the cells started to accumulate the muscle-specific IF protein desmin. As differentiation proceeds, vimentin expression is gradually downregulated and the protein becomes undetectable in mature myotubes, whereas desmin accumulates. These IFs are confined to the Z bands of myofibrils. On the other hand, desmin is already expressed in proliferating myoblasts derived from rat and mouse (Kaufman and Foster, 1988) and also in C2C12 myoblasts (Li et al., 1994; Abe et al., 1996). Vimentin markedly decreases during differentiation of C2C12 cells as in chicken myogenic cells (Li et al., 1994).

As loss of vimentin correlates with the nuclear deformation in SW-13 cells (Sarria et al., 1994), we examined the expression of vimentin in C2C12 cells during terminal differentiation. The proliferating myoblasts with smooth-surfaced nuclei had high levels of vimentin mRNA, whereas the 4-day myotubes had undetectable levels of the mRNA as revealed by northern blotting (see Fig. 4). Immunofluorescence microscopy also showed that vimentin was present in the myoblasts as typical IF networks (Fig. 3A a,b). By contrast, vimentin fluorescence was scarcely detected in the 4-day myotubes, which contained invaginated nuclei (Fig. 3A c,d). Immunoblotting with the mAb to vimentin showed that vimentin gradually decreased during terminal differentiation (Fig. 3B a). In the 4-day myotube culture, a low but distinct level of vimentin was detected. Most, if not all, of this band is probably ascribable to residual myoblasts in the myotube culture. Desmin was already present in proliferating myoblasts as detected by immunoblotting with the anti-desmin pAb (Fig. 3B b). Its amount increased to some degree during terminal differentiation.

Cells treated with sodium butyrate in the differentiation medium for 4 days were prevented from differentiation and contained smooth-surfaced nuclei as described above. They still accommodated vimentin filaments distributed throughout

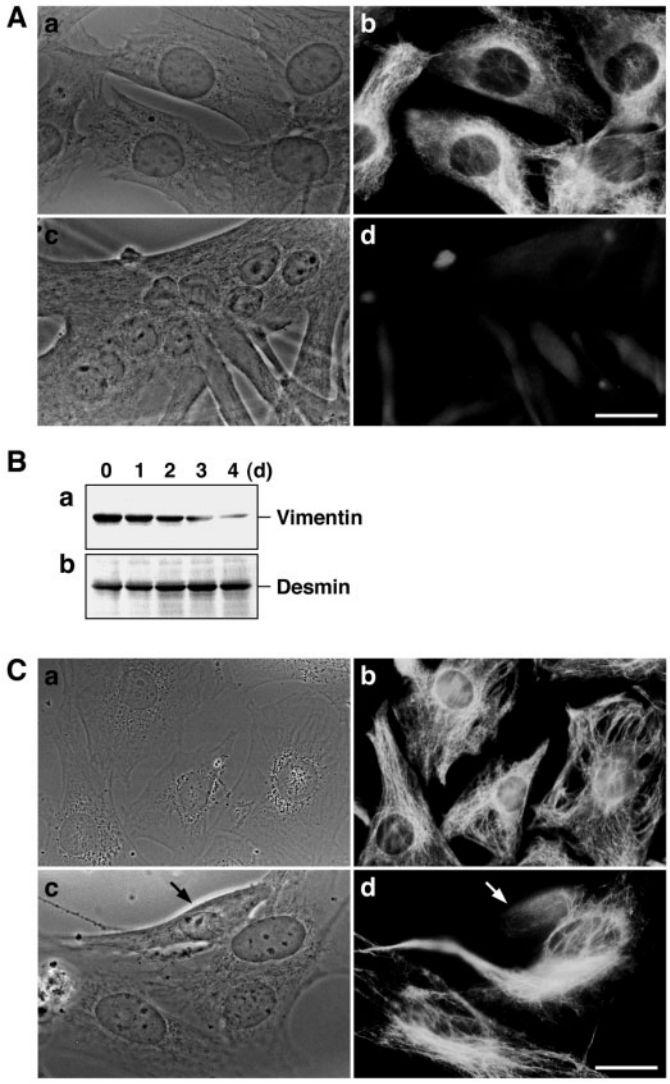

Fig. 3. Downregulation of vimentin in C2C12 myotubes and biochemically differentiated cells. (A) Disappearance of vimentin filaments during terminal differentiation. Phase-contrast images (a,c) and corresponding immunofluorescent images detecting vimentin (b,d) in C2C12 myoblasts (a,b) and myotubes (c,d). (B) A decrease in vimentin (a) and an increase in desmin (b) during terminal differentiation detected by immunoblotting. (C) Disappearance of vimentin filaments in biochemically differentiated mononucleated cells. Phase-contrast images (a,c) and corresponding immunofluorescent images detecting vimentin (b,d) of sodium butyrate-treated (a,b) or DMSO-treated (c,d) C2C12 cells. Cells were treated as described for Fig. 2B. Arrows indicate a biochemically differentiated cell, which has a invaginated nucleus and a markedly reduced number of vimentin filaments (c,d). Bar, 20 μm.

the cytoplasm (Fig. 3C a,b). The DMSO-treated, differentiation-blocked cells with smooth-surfaced nuclei also contained vimentin filament networks (Fig. 3C c,d). By contrast, biochemically differentiated cells with invaginated nuclei scarcely had any vimentin filaments (Fig. 3C c,d, arrows). These results appeared to support the idea that diminished vimentin expression is correlated with the nuclear invagination in these myogenic cells.

To examine this proposal, we transfected *vimentin* cDNA

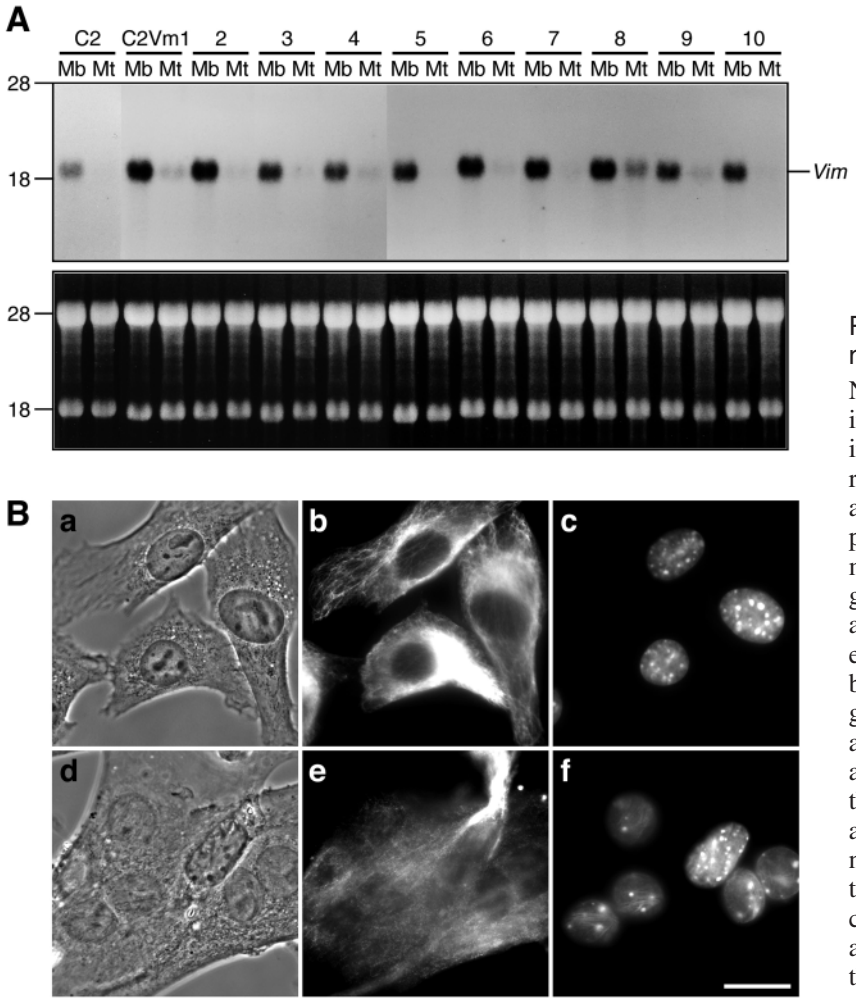

Fig. 4. Nuclear deformation in myotubes with forced expression of vimentin. (A) Northern blots detecting *vimentin* expression in C2C12 cells and the vimentin-transfected clones C2Vm1-10 (top). Ethidium bromide staining pattern of cytoplasmic RNAs in agarose gel electrophoresis showing the 28S and 18S rRNAs (bottom). (B) Nuclear shapes of C2Vm8 myoblasts (a-c) and myotubes (d-f). Phase-contrast images (a,d) and corresponding immunofluorescent staining of vimentin (b,e) and H33258 staining (c,f). Although C2Vm8 myotubes contain adequate vimentin filament networks, their nuclei have grooves and invaginations. Bar, 20 μm.

under the control of cytomegalovirus (CMV) promoter to C2C12 myoblasts and selected ten clones (C2Vm1-10) stably expressing the exogenous *vimentin*. The levels of vimentin mRNA in both myoblasts and 4-day myotube cultures were analyzed by northern blotting (Fig. 4A). The mRNA levels were more than several-fold higher in the myoblasts of these clones than in parental C2C12 myoblasts. The mRNA levels in myotubes of these clones were, however, prominently reduced. This is presumably because the CMV promoter is not highly active under low serum conditions such as in the differentiation medium. Yet, myotubes of the clone C2Vm8 had an mRNA level comparable to that of C2C12 myoblasts. C2Vm8 myoblasts contained normally distributed vimentin filaments and smooth-surfaced nuclei (Fig. 4B a-c). Although C2Vm8 myotubes contained adequate vimentin filament networks throughout the cytoplasm, almost all nuclei in the myotubes had grooves or invaginations (Fig. 4B d-f) like those in C2C12 myotubes (Fig. 2C). Myotubes of the other C2Vm clones also had nuclear deformations (data not shown). These results indicate that downregulation of vimentin during biochemical and terminal differentiation is not correlated with the formation of nuclear invagination in these myogenic cells.

Premyofibrils and myofibrils run along the nuclear grooves and invaginations

Next, to address whether actin filament bundles are involved in the formation of nuclear grooves and invaginations, we stained C2C12 myotubes with rhodamine-phalloidin, the anti-gizzard actin pAb and the anti-sarcomeric MyHC mAb. Rhodamine-phalloidin recognizes both muscle- and non-muscle-type actin filaments, whereas the anti-gizzard actin pAb absorbed with skeletal muscle actin specifically reacts with non-muscle actin (Abe et al., 1993). Some actin filament bundles detected by rhodamine-phalloidin staining ran along nuclear grooves or invaginations (Fig. 5A,B). Non-muscle actin filaments occasionally coexisted with these actin filament bundles penetrating the nucleus, but they were usually limited in number (Fig. 5A). In addition, penetrating actin filament bundles without non-muscle actin frequently existed (Fig. 5B). On the other hand, sarcomeric myosin filaments coexisted with the actin filament bundles running along the grooves or invaginations (Fig. 5C). Thus, these actin filament bundles are nascent myofibrils or premyofibrils and not stress fibers consisting of non-muscle actin and myosin. Furthermore, myofibrils with sarcomeric cross-striations detected by the staining with rhodamine-phalloidin and the anti-sarcomeric MyHC mAb also passed through nuclear grooves or invaginations (Fig. 5D). These premyofibrils and myofibrils often traversed multiple nuclei aligned in tandem (Fig. 5A-D). Taken together, these results imply that the premyofibrils and myofibrils penetrate the nuclei, and the penetration of these myofibrillar structures seems to be responsible for the formation of nuclear grooves or invaginations.

Some grooves or invaginations traversed the nucleus entirely, but others terminated within the nucleus. Actin and sarcomeric myosin were also present in the latter (Fig. 6A), suggesting that the myofibrillar structures are involved in both types of groove or invagination. Confocal microscopy showed that microtubules detected by the staining with the anti-β-tubulin mAb distributed throughout the cytoplasm of myotubes (Fig. 6B c). They were also often evenly distributed in the nuclear grooves or invaginations (Fig. 6B a,c), together with actin filament bundles (Fig. 6B b). Although the actin filament bundles were dense and thick, the microtubules were not dense in these regions. Accordingly, the presence of microtubules does not seem to have a critical effect on the formation of nuclear grooves or invaginations.

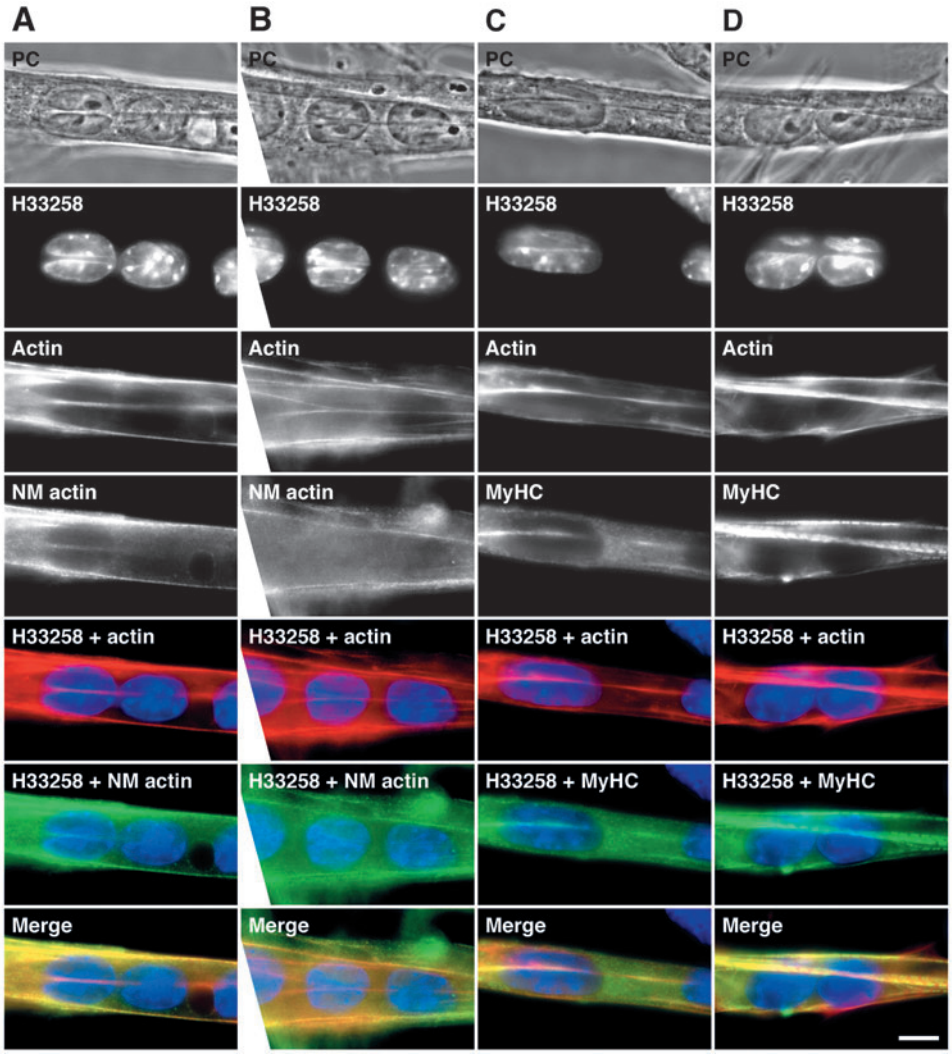

Fig. 5. Penetration of premyofibrils and myofibrils into the nuclear grooves and invaginations of myotubes. (A) Penetration of both muscle- and non-muscle-type actin-containing premyofibrils. (B) Penetration of muscle-type actin containing premyofibrils. Non-muscle-type actin is not present in the premyofibrils. (C) Penetration of actin- and myosin-containing premyofibrils. (D) Penetration of actin- and myosin-containing myofibrils with cross-striations. PC, phase-contrast images; H33258, nuclear staining with H33258; actin, total actin staining with rhodamine-phalloidin; NM actin, non-muscle actin staining with absorbed anti-gizzard actin pAb; MyHC, sarcomeric MyHC staining with the mAb A4.1025; H33258 + actin, H33258 + NM actin, H33258 + MyHC, doubly merged images; Merge, triply merged images. Bar, 10 μm.

Confocal optical sections of rhodamine-phalloidin and anti-sarcomeric MyHC staining (*XY* planes) and three-dimensional reconstitutions of the orthogonal planes derived from these sections (*XZ* and *YZ* planes) demonstrated that the myofibrils traversed both surface grooves (Fig. 7A) and intranuclear tubular invaginations (Fig. 7B,C) of the myotube nuclei. These myofibrillar structures traversed any areas of the nuclei, i.e. near-dorsal, central and near-ventral areas.

Optical sections of the staining with rhodamine-phalloidin together with the mAb to nucleoporin p62, a constituent protein of nuclear pore complexes, showed that the penetrating myofibrillar structures were surrounded by the nuclear envelope (Fig. 7D). Counterstaining with $DiOC_6(3)$ of the ER and the nuclear envelope connected to the ER also revealed that the myofibrillar structures were enclosed by the nuclear envelope (Fig. 7E). These results indicate that the myofibrillar structures stay in the cytoplasm and that they do not directly traverse the nucleoplasm.

Preformed myofibrillar structures cut horizontally into the nuclei

To examine how these myofibrillar structures penetrate the nuclei, we observed the living C2C12 myotubes containing H33342-stained nuclei and expressing EGFP-tagged α-actin by time-lapse microscopy. The nuclei without penetration of premyofibrils or myofibrils sometimes existed although they usually had grooves or invaginations that were curved or branched and did not run longitudinally. When premyofibrils or myofibrils ran over or under such nuclei (Fig. 8, time 0), they often cut into the nuclei horizontally and formed straight and longitudinal grooves or invaginations (Fig. 8, after time 0). The myofibrillar structures may press the nuclear envelope into the nuclei to form the grooves and invaginations, and thus the myofibrillar structures remain in the cytoplasm as stated above.

These results suggest that the myofibrillar structures play crucial roles in the formation of the straight and longitudinal nuclear grooves and invaginations. To confirm this, we added 10 mM BDM or 12 mM KCl to the differentiation medium. The addition of either BDM or KCl impairs the assembly of myofibrils without inhibiting myotube formation (Bandman and Strohman, 1982; Soeno et al., 1999) (T.O. et al., unpublished observations). C2C12 cells cultured for 4 days in the differentiation medium containing 10 mM BDM or 12 mM KCl formed myotubes. Essentially all nuclei in these myotubes had grooves or invaginations (Fig. 9A,B). Although the control myotubes in the normal differentiation medium often had straight and longitudinal nuclear grooves and invaginations traversed by the myofibrillar structures, the grooves or invaginations in the BDM- or KCl-treated myotubes were usually curved and branched and did not run longitudinally (Fig. 9A). The ratio of nuclei with straight and longitudinal grooves or invaginations was markedly reduced by exposure to BDM or KCl (Fig. 9B). These results corroborate the suggestion that the myofibrillar structures are responsible for the formation of the straight and longitudinal nuclear grooves

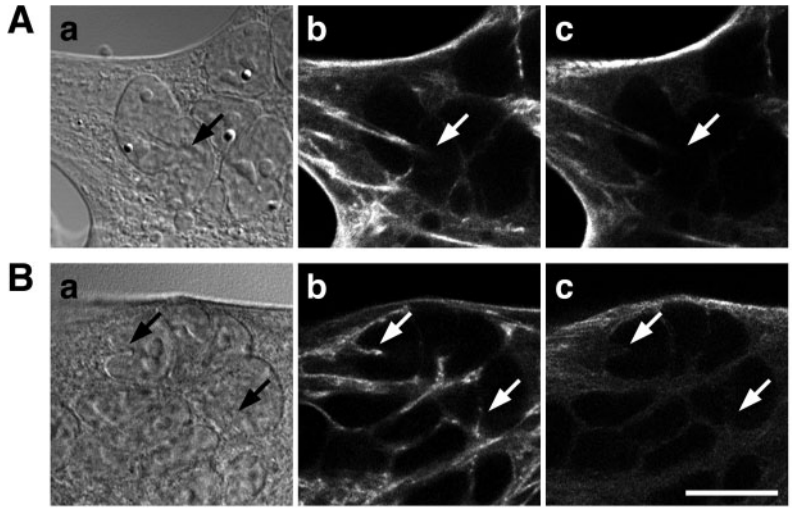

Fig. 6. Termination of myofibrillar tips within the nuclei and existence of microtubules in the nuclear invaginations. (A) Termination of myofibrillar tips within the nuclei. A differential interference contrast (DIC) image (a), corresponding rhodamine-phalloidin staining (b), and an immunofluorescent image detecting sarcomeric MyHC (c). Arrows indicate the tip of a premyofibril within the nucleus. (B) Existence of microtubules in the nuclear invaginations. A DIC image (a), corresponding rhodamine-phalloidin staining (b), and an immunofluorescent image detecting β-tubulin (c). Arrows indicate the nuclear invaginations containing premyofibrils and microtubules. Bar, 20 μm.

and invaginations. However, BDM or KCl treatment did not completely inhibit the formation of the straight and longitudinal grooves or invaginations. This is probably because incompletely organized myofibrils are formed as detected by electron microscopic observations even after treatment with these reagents (Soeno et al., 1999). Both BDM and KCl block the contraction of cultured muscle cells (Bandman and Strohman, 1982; Soeno et al., 1999). Thus, these results also demonstrate that contraction is not responsible for the formation of the curved or branched grooves and invaginations.

Sarcomeric protein mRNAs are located along the myofibrillar structures

One of the functions of the nuclear grooves and invaginations is thought to be communication between the nucleus and the cytoplasm, for example, mRNA export from the nucleus to the cytoplasm and protein import from the cytoplasm to the nucleus (Fricker et al., 1997; Collings et al., 2000). If this is true for the nuclear grooves and invaginations in myotubes, sarcomeric protein mRNAs, which are required for vigorous synthesis of sarcomeric proteins during myofibrillogenesis, may be transported along the traversing premyofibrils and myofibrils. To evaluate this possibility, we analyzed the location of sarcomeric protein mRNAs by FISH. Antisense probes of embryonic fast skeletal muscle *MyHC* and *α-actin* mRNA but not their sense probes showed clear hybridization signals in C2C12 myotubes. None of these probes showed signals in undifferentiated myoblasts (data not shown). Confocal optical sections of the myotubes with myofibrillar structures that traversed the nuclei revealed that the *MyHC* mRNA was preferentially associated with the traversing premyofibrils and myofibrils (Fig. 10A). *α-actin* mRNA was also associated with the traversing myofibrillar structures, though less tightly than *MyHC* mRNA (Fig. 10B). For both *MyHC* and *α-actin* mRNA, the association was particularly evident on the *XZ* planes, where the fluorescent particles representing mRNAs were aligned along myofibrillar structures at irregular intervals. The mRNAs were not preferentially associated with either A or I bands. These results may support the hypothesis that these traversing myofibrillar structures serve for the translocation of the sarcomeric protein mRNAs from the nucleus to the sites of sarcomeric protein synthesis.

Discussion

Here we have shown that the nuclei in C2C12 cells were transformed from smooth-surfaced ovals to intricate shapes with grooves and invaginations during terminal differentiation. This transformation was not specific for C2C12 cells because the nuclei in 10T1/2 fibroblasts converted to myogenic cells by the transfection with *MyoD* were also transformed to elaborate shapes after terminal differentiation. Furthermore, we showed that biochemically differentiated cells without cell fusion also contained deformed nuclei, but that the cells prevented from biochemical differentiation had smooth-surfaced nuclei even in the differentiation medium. These results indicate that not cell fusion but any one of the following responses associated with biochemical differentiation is sufficient for the nuclear deformation: (1) the expression of a battery of muscle-specific genes; (2) extinction of undifferentiated state-specific genes; or (3) muscle cell contraction.

One of the undifferentiated state-specific genes in myogenic cells is vimentin. Vimentin was highly expressed and typical vimentin filament networks extended in C2C12 myoblasts, whereas it was highly reduced and its filamentous networks were lost in the myotubes or in the biochemically differentiated cells. Human SW-13 cell clones lacking vimentin, which is the sole cytoplasmic IF protein in wild-type SW-13 cells, exhibit nuclear folds or invaginations (Sarria et al., 1994). Transfection of *vimentin* in these clones restores the smooth nuclear shape. Conversely, when vimentin-containing cell clones are transfected with a dominant-negative mutant of vimentin lacking its C-terminus, endogenous vimentin filaments are collapsed and the nuclei are invaginated. By contrast, our results showed that exogenous expression of *vimentin* in C2C12 myotubes did not recover the smooth nuclear shape. This result argues against the possibility that extinction of vimentin is responsible for the nuclear invaginations in differentiated C2C12 cells. In addition, although at most ~80% of the vimentin-positive and -negative clones of SW-13 cells have smooth and invaginated nuclear shapes, respectively, and the remainder have the opposite nuclear shapes (Sarria et al., 1994), almost all nuclei in C2C12 myoblasts and myotubes were smooth and invaginated, respectively. This also suggests that the nuclear shape of C2C12 cells cannot simply be explained by the presence or absence of vimentin. Mice deficient in *vimentin* gene ($Vim^{-/-}$) exhibit no obvious gross phenotypic alterations despite no compensatory expression of other IF proteins

(Colucci-Guyon et al., 1994). Cells derived from these mice do not appear to have deformed nuclei, which supports our results.

The convoluted or invaginated nuclei of striated and smooth muscle cells in muscle tissues have been well documented (Lane, 1965; Franke and Schinko, 1969). The deformation of the nuclei has been assumed to be generated either by mechanical forces through muscle contraction (Lane, 1965) or by intracellular ion changes (Franke and Schinko, 1969). Although C2C12 myotubes hardly contracted before day 4, they already

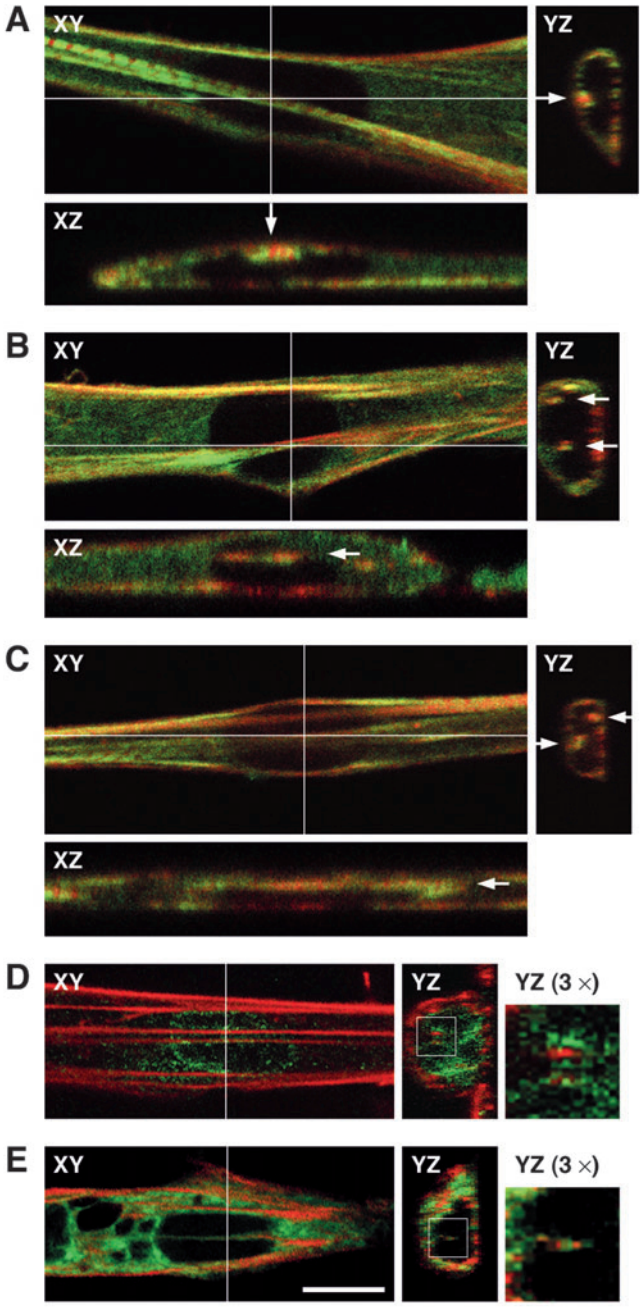

Fig. 7. Traversal of premyofibrils and myofibrils through the nuclear grooves and invaginations. Confocal optical sections (*XY* planes) and three-dimensional reconstitutions of the orthogonal planes derived from these sections (*XZ* and *YZ* planes). (A-C) Rhodamine-phalloidin (red) and anti-sarcomeric MyHC (green) staining of myofibrils passing through the nuclear grooves (A) and the nuclear invaginations (B,C). Arrows point to the traversing myofibrils. (D) Rhodamine-phalloidin (red) and anti-nucleoporin p62 (green) staining of myofibrillar structures and nuclear pore complexes, respectively. Boxed area in *YZ* plane is magnified three times. (E) Rhodamine-phalloidin (red) and $DiOC_6(3)$ (green) staining of myofibrillar structures and the ER together with the nuclear envelope, respectively. Bar, 10 μm.

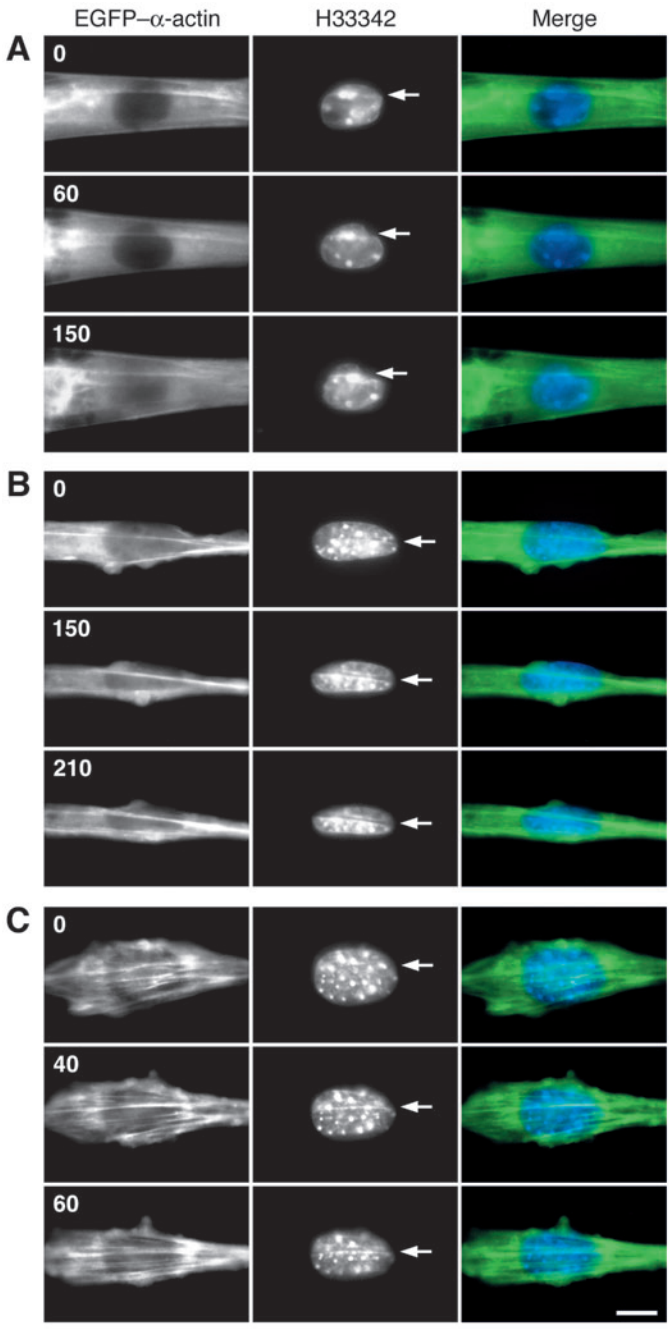

Fig. 8. Formation of the nuclear grooves and invaginations by myofibrillar structures horizontally cutting into the nuclei. (A-C) The nuclei of living C2C12 myotubes expressing EGFP-tagged α-actin were stained with H33342. The fluorescence of EGFP and H33342 was recorded at intervals of 20-30 minutes at 37°C. Shown are selected images of three cells by time-lapse microscopy. The numbers indicate minutes after starting the observation. Arrows point to the positions of nuclei, where myofibrillar structures enter horizontally. Bar, 10 μm.

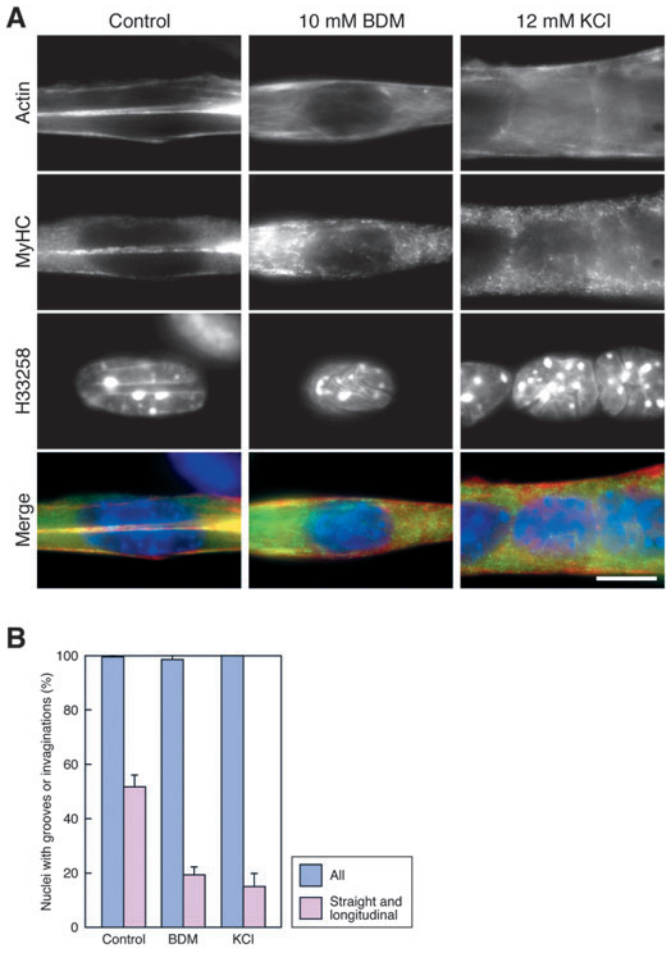

Fig. 9. Reduction of straight and longitudinal nuclear grooves and invaginations by preventing myofibrillogenesis. C2C12 myoblasts were cultured for 4 days in the differentiation medium (control) or the medium containing 10 mM BDM or 12 mM KCl to prevent myofibril assembly. (A) Staining of the myotubes with rhodamine-phalloidin (actin), anti-MyHC mAb, and H33258 along with their merged images. (B) Ratio of all the nuclei in myotubes with grooves or invaginations and that of the nuclei with straight and longitudinal grooves or invaginations. More than 200 nuclei were counted in each experiment. The values are mean±s.d. of three experiments. Bar, 10 μm.

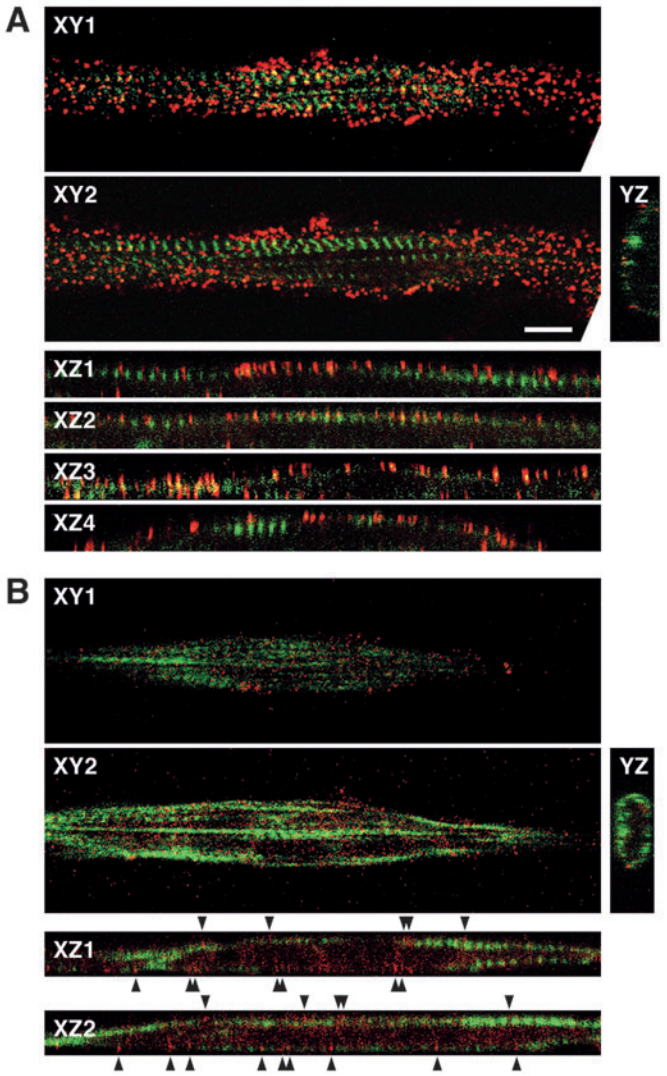

Fig. 10. Association of sarcomeric protein mRNAs with myofibrillar structures traversing through the nuclear invaginations. Confocal optical sections of FISH detecting sarcomeric protein mRNAs (red) and Alexa 488-phalloidin (green) staining (*XY* planes) and three-dimensional reconstitutions of the orthogonal planes derived from these sections (*XZ* and *YZ* planes). (A) FISH of embryonic fast skeletal muscle *MyHC* mRNA. Different focal planes (*XY*1 and 2; *XZ*1-4) of a myotube are shown. Association of the mRNA with the myofibrillar structures is more evident on the *XZ* planes. Penetration of myofibrils into the nuclear invaginations is evident on the *YZ* plane. (B) FISH of skeletal muscle *α-actin* mRNA. Different focal planes (*XY*1 and 2; *XZ*1 and 2) of a myotube are shown. Arrowheads on the *XZ* planes indicate association of the mRNA with the myofibrillar structures. Bar, 10 μm.

had grooved or invaginated nuclei. In addition, despite the fact that the biochemically differentiated cells without cell fusion never contracted, they also had deformed nuclei. Moreover, although both BDM and KCl block the contraction of cultured muscle cells (Bandman and Strohman, 1982; Soeno et al., 1999), the treatment of C2C12 myotubes with BDM or KCl did not interfere with the formation of curved or branched nuclear grooves and invaginations. Consequently, the nuclear deformation is not ascribed to mechanical forces generated by contraction, at least in C2C12 cells. On the other hand, Ca^{2+} is required for both muscle-specific protein accumulation and cell fusion of mammalian skeletal myocytes (Konieczny et al., 1982; Endo and Nadal-Ginard, 1987). Therefore, Ca^{2+} might be prerequisite for the nuclear deformation in C2C12 cells. More recent studies have shown that Ca^{2+} is released from the nuclear envelope of nuclear invaginations or tubules into the nucleoplasm but not to the cytoplasm in C6 glioma cells (Lui et al., 1998). Accordingly, it remains to be determined whether Ca^{2+} released from the sarcoplasmic reticulum into the cytoplasm, or from the nuclear envelope into the nucleoplasm, or both, are responsible for the nuclear deformation in differentiated C2C12 cells.

At prophase in mitosis, elongating astral microtubules penetrate into the nuclei to give rise to nuclear folds and invaginations (Georgatos et al., 1997). As a consequence, the microtubules generate mechanical tension and induce tearing

of the nuclear lamina, leading to nuclear envelope breakdown (Beaudouin et al., 2002). The minus-end-directed microtubule motor dynein and dynactin complex concentrated on the nuclear envelope may facilitate nuclear envelope breakdown by pulling nuclear membranes and associated proteins toward the centrosomes along astral microtubules (Salina et al., 2002). In the invaginations of myotubes, however, microtubules were present but not concentrated. Thus, these microtubules by themselves may not be sufficient to produce mechanical tension to form nuclear invaginations. In addition, because myotubes and biochemically differentiated cells are arrested in G_0 phase and do not resume mitosis upon mitogen stimulation, centrosomes are not formed and nuclear envelope breakdown does not occur in these cells (Endo and Nadal-Ginard, 1986; Endo and Nadal-Ginard, 1998). Therefore, microtubules cannot mediate nuclear invaginations leading to the tearing of nuclear lamina in these quiescent cells.

Nuclear grooves and invaginations of some types of animal and plant cells contain actin filaments (Clubb and Locke, 1998; Collings et al., 2000). Swiss 3T3 cells have two kinds of invagination: branched invaginations radiating horizontally through the nucleoplasm and those running perpendicularly to the substrate. The former contain actin filaments, which may be associated with the nuclear membrane (Clubb and Locke, 1998). On the other hand, nuclear invaginations of onion epidermal cells contain thick actin filament bundles (Collings et al., 2000). Accordingly, actin filaments are also likely to be responsible for the formation of nuclear grooves and invaginations. These actin filaments inevitably consist of non-muscle actin, and it is not known whether myosin is present in these actin filament bundles. We have shown that premyofibrils and myofibrils, which consist of muscle α-actin and myosin, also participate in the formation of nuclear invaginations. Because only limited amounts of non-muscle actin, if any, were present in the traversing premyofibrils, non-muscle actin and possibly non-muscle myosin as well, may not be essential for the formation of invaginations in the myotubes. Alternatively, actin filament bundles or stress fibers consisting of non-muscle actin and myosin may be transiently involved in the formation of invaginations at early stages of differentiation and replaced by the myofibrillar structures afterwards. As the myofibrillar structures usually run straight and parallel to the long axis of myotubes, they seem to be responsible for the formation of nuclear grooves and invaginations that traverse or penetrate the nucleus relatively straight and longitudinally. Indeed, the abrogation of myofibrillogenesis with BDM or KCl markedly reduced the number of the nuclei with straight and longitudinal grooves or invaginations. Furthermore, time-lapse microscopy clearly showed that preformed myofibrillar structures horizontally cut into the nuclei to form the straight and longitudinal grooves or invaginations. However, some nuclei also had grooves and invaginations that were curved or branched and did not run longitudinally. The mechanisms for the formation of these grooves and invaginations remain to be elucidated.

mRNAs are transported to be localized within the cytoplasm as ribonucleoprotein (RNP) complexes along actin microfilaments or microtubules by associated motor proteins (Bassell et al., 1999; Jansen, 2001; Tekotte and Davis, 2002; López de Heredia and Jansen, 2004). The RNP complexes contain zipcode-binding proteins recognizing specific 'zipcode' sequences in the 3′-untranslated region of mRNAs (Jansen, 2001; Farina and Singer, 2002). In developing and regenerating skeletal muscle, association of polysomes or ribosomes with myofibrils has been well documented (Larson et al., 1969; Larson et al., 1973; Horne and Hesketh, 1990; Gauthier and Mason-Savas, 1993). These polysomes are preferentially aligned along or between the thick filaments. Sarcomeric protein mRNAs generally accumulate in regions of myofibrillar growth and repair as well as around transcriptionally active myonuclei (Russell and Dix, 1992). Typically, mRNAs of several myofibrillar and costamere proteins, including MyHC, connectin/titin, nebulin, desmin, vimentin and vinculin, are periodically located in myofibrils or costameres (Aigner and Pette, 1990; Morris and Fulton, 1994; Fulton and Alftine, 1997). We have shown here that mRNAs of *MyHC* and *α-actin* are associated with premyofibrils and myofibrils running along the nuclear grooves and invaginations. Considering the mechanisms of mRNA translocation along microfilaments or microtubules, these mRNAs seem to be translocated from the nuclei to the cytoplasmic destination along these myofibrillar structures. As mature myofibrils are actively reconstructed from premyofibrils and elongated during differentiation, satisfactory amounts of sarcomeric protein mRNAs and translated proteins are required for the myofibrillogenesis. The nuclear grooves and invaginations seem to be pertinent to the actively progressing myofibrillogenesis because they substantially increase the surface area of the nucleus to elevate the efficiency of mRNA transport from the nucleus to the cytoplasm through nuclear pore complexes.

A variety of mRNAs are transported along microtubules by the motor proteins, kinesin I and dynein, in vertebrates as well as in *Drosophila* eggs and embryos (Jansen, 2001; Tekotte and Davis, 2002; López de Heredia and Jansen, 2004). By contrast, several mRNAs in yeast are transported along actin filaments by myosin V class motors. On the other hand, *β-actin* mRNA associated with the zipcode-binding protein ZBP1 is transported by myosin IIB along microfilaments to the leading edge in chicken fibroblasts (Latham et al., 2001; Oleynikov and Singer, 2003). When mRNAs of *MyHC* and *α-actin* are transported along the myofibrils traversing the nuclei, the functional motors may be myosin II constituting the myofibrils, as for transport of *β-actin* mRNA, rather than microtubule-linked motors. Indeed, neither kinesin I nor dynein was colocalized with the myofibrils (data not shown). The zipcode-binding proteins participating in the transport of these mRNAs remain to be identified. Furthermore, it would be intriguing to examine whether all the sacromeric protein mRNAs and also housekeeping protein mRNAs are transported along the traversing myofibrils. In any case, the myotubes containing the grooved or invaginated nuclei traversed by the myofibrillar structures may provide one of the model systems for analysis of the mechanisms of mRNA transport from the nucleus.

We dedicate this paper to Dr Koscak Maruyama, who died last year. This work was partly supported by Grants-in-Aid from the Ministry of Education, Culture, Sports, Science, and Technology of Japan and by the Research Grants (11B-1 and 14B-4) for Nervous and Mental Disorders from the Ministry of Health, Labor, and Welfare of Japan.

References

Abe, H., Nagaoka, R. and Obinata, T. (1993). Cytoplasmic localization and nuclear transport of cofilin in cultured myotubes. *Exp. Cell Res.* **206**, 1-10.

Abe, M., Saitoh, O., Nakata, H., Yoda, A. and Matsuda, R. (1996). Expression

of neurofilament proteins in proliferating C2C12 mouse skeletal muscle cells. *Exp. Cell Res.* **229**, 48-59.

Aigner, S. and Pette, D. (1990). In situ hybridization of slow myosin heavy chain mRNA in normal and transforming rabbit muscles with the use of a nonradioactively labeled cRNA. *Histochemistry* **95**, 11-18.

Bader, D., Masaki, T. and Fischman, D. A. (1982). Immunochemical analysis of myosin heavy chain during avian myogenesis in vivo and in vitro. *J. Cell Biol.* **95**, 763-770.

Bandman, E. and Strohman, R. C. (1982). Increased K^+ inhibits spontaneous contractions and reduced myosin accumulation in cultured chick myotubes. *J. Cell Biol.* **93**, 698-704.

Bassell, G. J., Zhang, H., Byrd, A. L., Femino, A. M., Singer, R. H., Taneja, K. L., Lifshitz, L. M., Herman, I. M. and Kosik, K. S. (1998). Sorting of β-actin mRNA and protein to neurites and growth cones in culture. *J. Neurosci.* **18**, 251-265.

Bassell, G. J., Oleynikov, Y. and Singer, R. H. (1999). The travels of mRNAs through all cells large and small. *FASEB J.* **13**, 447-454.

Beaudouin, J., Gerlich, D., Daigle, N., Eils, R. and Ellenberg, J. (2002). Nuclear envelope breakdown proceeds by microtubule-induced tearing of the lamina. *Cell* **108**, 83-96.

Bennett, G. S., Fellini, S. A., Toyama, Y. and Holtzer, H. (1979). Redistribution of intermediate filament subunits during skeletal myogenesis and maturation in vitro, *J. Cell Biol.* **82**, 577-584.

Bernhard, W. and Granboulan, N. (1963). The fine structure of the cancer cell nucleus. *Exp. Cell Res.* **9**, 19-53.

Blau, H. M., Chiu, C.-P. and Webster, C. (1983). Cytoplasmic activation of human nuclear genes in stable heterocaryones. *Cell* **32**, 1171-1180.

Bourgeois, C. A., Hemon, D. and Bouteille, M. (1979). Structural relationship between the nucleolus and the nuclear envelope. *J. Ultrastruct. Res.* **68**, 328-340.

Clubb, B. H. and Locke, M. (1998). 3T3 cells have nuclear invaginations containing F-actin. *Tissue Cell* **30**, 684-691.

Collings, D. A., Carter, C. N., Rink, J. C., Scott, A. C., Wyatt, S. E. and Allen, N. S. (2000). Plant nuclei can contain extensive grooves and invaginations. *Plant Cell* **12**, 2425-2439.

Colucci-Guyon, E., Portier, M.-M., Dunia, I., Paulin, D., Pournin, S. and Babinet, C. (1994). Mice lacking vimentin develop and reproduce without an obvious phenotype. *Cell* **79**, 679-694.

Davis, R. L., Weintraub, H. and Lassar, A. B. (1987). Expression of a single transfected cDNA converts fibroblasts to myoblasts. *Cell* **51**, 987-1000.

Endo, T. (1992). SV40 large T inhibits myogenic differentiation partially through inducing c-*jun*. *J. Biochem.* **112**, 321-329.

Endo, T. and Masaki, T. (1982). Molecular properties and functions in vitro of chicken smooth-muscle α-actinin in comparison with those of striated-muscle α-actinins. *J. Biochem.* **92**, 1457-1468.

Endo, T. and Masaki, T. (1984). Differential expression and distribution of chicken skeletal- and smooth-muscle-type α-actinins during myogenesis in culture. *J. Cell Biol.* **99**, 2322-2332.

Endo, T. and Nadal-Ginard, B. (1986). Transcriptional and posttranscriptional control of c-*myc* during myogenesis: its mRNA remains inducible in differentiated cells and does not suppress the differentiated phenotype. *Mol. Cell. Biol.* **6**, 1412-1421.

Endo, T. and Nadal-Ginard, B. (1987). Three types of muscle-specific gene expression in fusion-blocked rat skeletal muscle cells: translational control in EGTA-treated cells. *Cell* **49**, 515-526.

Endo, T. and Nadal-Ginard, B. (1998). Reversal of myogenic terminal differentiation by SV40 large T antigen results in mitosis and apoptosis. *J. Cell Sci.* **111**, 1081-1093.

Farina, K. L. and Singer, R. H. (2002). The nuclear connection in RNA transport and localization. *Trends Cell Biol.* **12**, 466-472.

Franke, W. W. and Schinko, W. (1969). Nuclear shape in muscle cells. *J. Cell Biol.* **42**, 326-331.

Fricker, M., Hollinshead, M., White, N. and Vaux, D. (1997). Interphase nuclei of many mammalian cell types contain deep, dynamic, tubular membrane-bound invaginations of the nuclear envelope. *J. Cell Biol.* **136**, 531-544.

Fulton, A. B. and Alftine, C. (1997). Organization of protein and mRNA for titin and other myofibril components during myofibrillogenesis in cultured skeletal muscle. *Cell Struct. Funct.* **22**, 51-58.

Gauthier, G. F. and Mason-Savas, A. (1993). Ribosomes in the skeletal muscle filament lattice. *Anat. Rec.* **237**, 149-156.

Georgatos, S. D., Pyrpasopoulou, A. and Theodoropoulos, P. A. (1997). Nuclear envelope breakdown in mammalian cells involves stepwise lamina disassembly and microtubule-drive deformation of the nuclear membrane. *J. Cell Sci.* **110**, 2129-2140.

Horne, Z. and Hesketh, J. (1990). Immunological localization of ribosomes in striated rat muscle. *Biochem. J.* **268**, 231-236.

Hoshino, M. (1961). The deep invagination of the inner nuclear membrane into the nucleoplasm in the ascites hepatoma cells. *Exp. Cell Res.* **24**, 606-609.

Inagaki, M., Matsuoka, Y., Tsujimura, K., Ando, S., Tokui, T., Takahashi, T. and Inagaki, N. (1996). Dynamic property of intermediate filaments: regulation by phosphorylation. *Bioessays* **18**, 481-487.

Jansen, R.-P. (2001). mRNA localization: message on the move. *Nat. Rev. Mol. Cell Biol.* **2**, 247-256.

Kamei, H. (1994). Relationship of nuclear invaginations to perinuclear rings composed of intermediate filaments in MIA PaCa-2 and some other cells. *Cell Struct. Funct.* **19**, 123-132.

Kaufman, S. J. and Foster, R. (1988). Replicating myoblasts express a muscle-specific phenotype. *Proc. Natl. Acad. Sci. USA* **85**, 9606-9610.

Konieczny, S. F., McKay, J. and Coleman, J. R. (1982). Isolation and characterization of terminally differentiated chicken and rat skeletal muscle myoblasts. *Dev. Biol.* **91**, 11-26.

Lane, B. P. (1965). Alterations in the cytoplasmic details of intestinal smooth muscle cells in various stages of contraction. *J. Cell Biol.* **27**, 199-213.

Larson, P. F., Hudgson, P. and Walton, J. N. (1969). A morphological relationship of polyribosomes and myosin filaments in developing and regenerating skeletal muscle. *Nature* **222**, 1168-1169.

Larson, P. F., Fulthorpe, J. J. and Hudgson, P. (1973). The alignment of polysomes along myosin filaments in developing myotubes. *J. Anat.* **116**, 327-334.

Latham, V. M., Jr, Yu, E. H. S., Tullio, A. N., Adelstein, R. S. and Singer, R. H. (2001). A Rho-dependent signaling pathway operating through myosin localizes β-actin mRNA in fibroblasts. *Curr. Biol.* **11**, 1010-1016.

Li, H., Choudhary, S. K., Milner, D. J., Munir, M. I., Kuisk, I. R. and Capetanaki, Y. (1994). Inhibition of desmin expression blocks myoblast fusion and interferes with the myogenic regulators MyoD and myogenin. *J. Cell Biol.* **124**, 827-841.

López de Heredia, M. and Jansen, R.-P. (2004). mRNA localization and the cytoskeleton. *Curr. Opin. Cell Biol.* **16**, 80-85.

Lui, P. P. Y., Lee, C. Y., Tsang, D. and Kong, S. K. (1998). Ca^{2+} is released from the nuclear tubular structure into nucleoplasm in C6 glioma cells after stimulation with phorbol ester. *FEBS Lett.* **432**, 82-87.

Matsumoto, K., Asano, T. and Endo, T. (1997). Novel small GTPase M-Ras participates in reorganization of actin cytoskeleton. *Oncogene* **15**, 2409-2417.

Morris, E. J. and Fulton, A. B. (1994). Rearrangement of mRNAs for costamere proteins during costamere development in cultured skeletal muscle from chicken. *J. Cell Sci.* **107**, 377-386.

Oleynikov, Y. and Singer, R. H. (2003). Real-time visualization of ZBP1 association with β-actin mRNA during transcription and localization. *Curr. Biol.* **13**, 199-207.

Reznikoff, C. A., Brankow, D. W. and Heidelberger, C. (1973). Establishment and characterization of a cloned line of C3H mouse embryo cells sensitive to postconfluence inhibition of division. *Cancer Res.* **33**, 3231-3238.

Russell, B. and Dix, D. J. (1992). Mechanisms for intracellular distribution of mRNA: in situ hybridization studies in muscle. *Am. J. Physiol.* **262**, C1-C8.

Salina, D., Bodoor, K., Eckley, D. M., Schroer, T. A., Rattner, J. B. and Burke, B. (2002). Cytoplasmic dynein as a facilitator of nuclear envelope breakdown. *Cell* **108**, 97-107.

Sarria, A. J., Lieber, J. G., Nordeen, S. K. and Evans, R. M. (1994). The presence or absence of a vimentin-type intermediate filament network affects the shape of the nucleus in human SW-13 cells. *J. Cell Sci.* **107**, 1593-1607.

Soeno, Y., Shimada, Y. and Obinata, T. (1999). BDM (2,3-butanedione monoxime), an inhibitor of myosin-actin interaction, suppresses myofibrillogenesis in skeletal muscle cells in culture. *Cell Tissue Res.* **295**, 307-316.

Tekotte, H. and Davis, I. (2002). Intracellular mRNA localization: motors move messages. *Trends Genet.* **18**, 636-642.

Tokuyasu, K. T., Maher, P. A. and Singer, S. J. (1984). Distribution of vimentin and desmin in developing chick myotubes in vivo. I. Immunofluorescence study. *J. Cell Biol.* **98**, 1961-1972.

Webster, C., Silberstein, L., Hays, A. P. and Blau, H. M. (1988). Fast muscle fibers are preferentially affected in Duchenne muscular dystrophy. *Cell* **52**, 503-513.

Wood, L., Theriault, N. and Vogeli, G. (1989). Vimentin cDNA clones covering the complete intermediate-filament protein are found in an EHS tumor cDNA library. *Gene* **76**, 171-175.

Yaffe, D. and Saxel, O. (1977). Serial passaging and differentiation of myogenic cells isolated from dystrophic mouse muscle. *Nature* **270**, 725-727.